

Stochastic Dynamics of Sea Surface Winds

Adam Hugh Monahan

*School of Earth and Ocean Sciences, University of Victoria
PO Box 3055 STN CSC Victoria, BC, Canada V8W 3P6
monahana@uvic.ca*

ABSTRACT

The probability distribution of sea surface winds (both vector winds and wind speed) is considered. The observed moment fields, estimated from SeaWinds scatterometer data, are shown to be characterised by non-trivial relationships such that higher-order moments are functionally dependent on lower-order moments. The physical mechanisms underlying these relationships are elucidated using a simple stochastic model derived from boundary layer dynamics. A class of more quantitatively accurate empirical models for the probability distribution of sea surface winds is discussed.

1 Introduction

Models of the probability distribution of sea surface winds (both vector winds and wind speed) play a central role in a number of problems in meteorology, oceanography, and climate; these include wind power meteorology (Petersen et al., 1998), remote sensing of sea surface winds (e.g. Meissner et al., 2001), and estimates of air/sea exchanges of heat, momentum, moisture, and gases (e.g. Thompson et al., 1983; Isemer and Hasse, 1991; Wanninkhof et al., 2002). For example, turbulent air/sea fluxes depend on eddy-averaged quantities such as the friction or piston velocities, which for many applications are parameterised in terms of the sea surface wind speed. Because of the nonlinear dependence on sea surface wind speed of these bulk formulae for air/sea fluxes, their spatial or temporal averages will not generally equal the fluxes associated with the average surface wind speed. In particular, grid-scale averages of these fluxes in general circulation models (GCMs) will not equal the fluxes associated with grid-scale winds. Furthermore, the average wind speed is not generally equal to the magnitude of the average vector wind: highly variable but isotropic fluctuations in the vector wind will be associated with a large average speed but yield a mean vector with small amplitude (e.g. Mahrt and Sun, 1995). The surface wind fields produced by GCMs represent grid-scale averaged vector winds, but grid-scale wind speed distributions are required to diagnose air/sea fluxes. Improvements to calculations of the fluxes can be obtained through the use of parameterisations of the probability density function (pdf) of sea surface wind speed which take as input grid-scale variables (e.g. Cakmur et al., 2004).

A new era in the study of the study of sea surface winds began with the advent of satellite anemometry, using both active and passive remote sensing devices (e.g. Kelly, 2004). Satellite-borne instruments have provided global observations of sea surface winds with unprecedentedly high resolution in space and time, allowing statistically significant characterisation of the pdfs of surface wind speeds in previously poorly-sampled oceanic regions. In particular, the SeaWinds scatterometer mounted on the QuikSCAT satellite has provided measurements of sea surface vector winds with daily resolution from mid-1999 to the present.

This study will use this high resolution dataset to characterise the pdfs of the sea surface vector winds and wind speed, through a study of the lowest moments (mean, standard deviation, and skewness). We will show that these pdfs are characterised by non-trivial relationships between the moments, such that higher-order moments can be predicted to a high degree of accuracy from low-order moments. Using a simple stochastic model

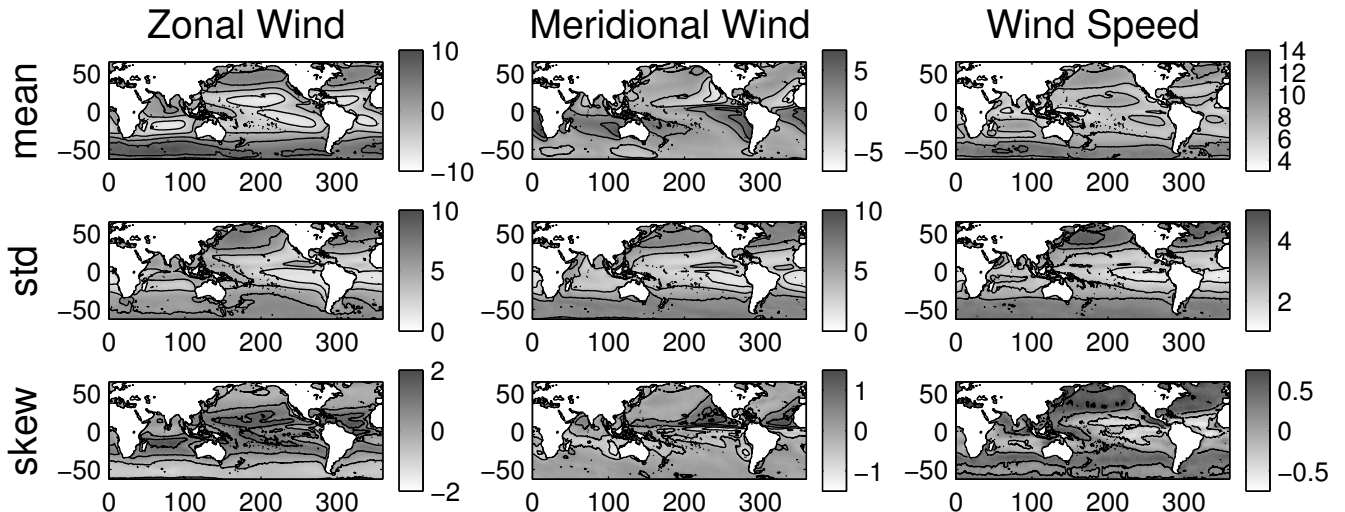


Figure 1: Mean, standard deviation, and skewness fields of the SeaWinds zonal wind, meridional wind, and wind speed.

derived via a clear sequence of approximations from boundary-layer momentum equations, it will be seen that these relationships arise as a consequence of the constraints placed on the sea surface wind pdfs by the physics of the boundary layer. In particular, the nonlinear dependence of the surface drag on the wind speed is seen to be essential for accounting for these relationships between moments. This model is too simple to be quantitatively useful, so an empirical model of the pdf of the surface winds is constructed which exploits the observed relationships between the low-order moments of the sea surface vector winds. This empirical model will be demonstrated to be more quantitatively accurate than similar models which have neglected non-Gaussian structure in the surface vector wind.

2 Observed Moments of Sea Surface Winds

The sea surface wind dataset considered in this study consists of Level 3.0 gridded daily SeaWinds scatterometer 10-m zonal and meridional wind observations from the NASA QuikSCAT satellite (Jet Propulsion Laboratory, 2001), available on a $1/4^\circ \times 1/4^\circ$ grid from July 19, 1999 to the present (March 15, 2005 for the present study).¹ The SeaWinds data have been extensively compared with buoy and ship measurements of surface winds (Ebuchi et al., 2002; Bourassa et al., 2003); the root-mean-squared errors of the remotely sensed wind speed and direction are both found to be dependent on wind speed, with average values of $\sim 1\text{ms}^{-1}$ and $\sim 20^\circ$ respectively. Because raindrops are effective scatterers of microwaves in the wavelength band used by SeaWinds, rainfall can lead to errors in estimates of sea surface winds. The SeaWinds Level 3.0 dataset flags those datapoints that are estimated as likely to have been corrupted by rain (Jet Propulsion Laboratory, 2001); these datapoints have been excluded from the present analysis. No further processing of the data, such as filtering or removing the annual cycle, was carried out on this dataset.

The mean, standard deviation, and skewness fields of the SeaWinds sea surface zonal wind (U), meridional wind (V), and wind speed (w) are presented in Figure 1. The skewness of a random variable x is the normalised third-order moment,

$$\text{skew}(x) = \frac{\text{mean}((x - \text{mean}(x))^3)}{\text{std}^3(x)}. \quad (1)$$

¹These data are available for download from the NASA JPL Distributed Active Archive Center, <http://podaac.jpl.nasa.gov>.

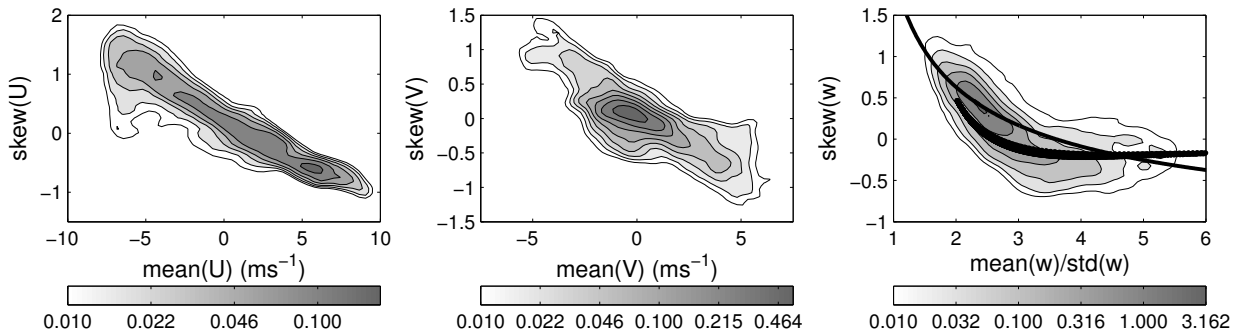


Figure 2: Kernel density estimates (contoured on a logarithmic scale) of the joint pdfs of $\text{mean}(U)$ with $\text{skew}(U)$ (left panel), $\text{mean}(V)$ with $\text{skew}(V)$ (centre panel), and $\text{mean}(w)/\text{std}(w)$ with $\text{skew}(w)$ (right panel). In the rightmost panel, the thin line is the curve predicted for a Weibull variable and the thick line is the curve predicted by the stochastic boundary layer model (9)-(10).

The $\text{mean}(U)$ field displays the familiar tropical easterlies and midlatitude westerlies, while the $\text{mean}(V)$ field shows strong flow only on the eastern flanks of the subtropical highs. The $\text{std}(U)$ and $\text{std}(V)$ fields display variability minima in the tropics and subtropics, and variability maxima in the storm tracks. The $\text{skew}(U)$ field is generally positive in the tropics and negative in the midlatitudes, while the $\text{skew}(V)$ field is generally small except along the eastern flanks of the subtropical highs, where skewness is positive in the Northern Hemisphere and negative in the Southern Hemisphere. Large values of $\text{mean}(w)$ occur in the westerly belts of the Northern and Southern Hemispheres; secondary maxima in the easterly belt lie along the equatorward flanks of the subtropical highs. Minima of $\text{mean}(w)$ occur in the equatorial doldrums and subtropical horse latitudes. The standard deviation of w is largest in the midlatitude extratropics (in the storm tracks), and generally decreases towards the equator, but with a local maximum along the Intertropical Convergence Zone (ITCZ). In general, w is positively skewed in the extratropics and negatively skewed in the tropics. Major exceptions to this pattern are the band of positively skewed wind speeds over the tropical Indian Ocean and Western Pacific, where mean wind speeds are small; and over the Southern Ocean, where the skewness of w is generally close to zero.

Linear relationships between $\text{mean}(U)$ and $\text{skew}(U)$, and between $\text{mean}(V)$ and $\text{skew}(V)$, are evident from Figure 1: positive (negative) mean wind components are associated with negative (positive) skewness. This spatial anticorrelation is further illustrated in Figure 2, which presents kernel density estimates of the joint pdfs of $\text{mean}(U)$ with $\text{skew}(U)$, and of $\text{mean}(V)$ with $\text{skew}(V)$. The spatial correlation coefficients between the mean and skewness fields of the zonal and meridional wind components are respectively -0.91 and -0.79 (with essentially no seasonal variability).

A number of empirical studies have demonstrated that the pdf sea surface wind speeds is well-approximated by the Weibull distribution, a unimodal distribution characterised by two parameters (see Monahan (2005a) for a literature review and a discussion of the Weibull distribution). A relevant characteristic of a Weibull variable x is that $\text{skew}(x)$ is uniquely determined by the ratio $\text{mean}(x)/\text{std}(x)$. Figure 2 displays a kernel density estimate of the joint pdf of $\text{mean}(w)/\text{std}(w)$ with $\text{skew}(w)$ from the SeaWinds observations, along with a plot of $\text{skew}(w)$ as a function of $\text{mean}(w)/\text{std}(w)$ for a Weibull variable. Evidently, for both the observations and the Weibull variable, $\text{skew}(w)$ is a concave upward function of the ratio $\text{mean}(w)/\text{std}(w)$, such that the function is positive for small values of this ratio and negative for large values. The Weibull curve is not a perfect characterisation of this relationship between moments: the slope of the observed relationship between $\text{skew}(w)$ and the ratio $\text{mean}(w)/\text{std}(w)$ is steeper than that of the Weibull curve for low values of the ratio and shallower for larger values of the ratio. Nevertheless, the Weibull distribution is a good approximation to the pdf of w as it shares with observations a characteristic relationship between moments.

These relationships between moments are not an artifact of the SeaWinds data; qualitatively similar relationships are found in other sea surface wind datasets (Monahan, 2004b, 2005b).

3 Sea Surface Wind pdfs: Stochastic Boundary Layer Model

To obtain a physical understanding of the relationships between moments characterising the observed pdfs of sea surface winds, we will consider the simple stochastic model for boundary-layer winds introduced in Monahan (2004b) and studied in more detail in Monahan (2004a, 2005a). This model has been demonstrated to be in good qualitative agreement with empirical stochastic models of sea surface winds (Sura, 2003; Sura and Sardeshmukh, 2004). At any given location over the sea surface, we will define the surface wind vector components relative to a local coordinate system:

$$\begin{aligned} u &= \text{wind component along local mean wind vector} \\ v &= \text{wind component across local mean wind vector (positive to the left)} \end{aligned}$$

Denoting the vector wind by $\mathbf{u} = (u, v)$, the eddy-averaged horizontal momentum equation can be written

$$\frac{\partial \mathbf{u}}{\partial t} + \mathbf{u} \cdot \nabla \mathbf{u} = -\frac{1}{\rho} \nabla p - f \hat{\mathbf{k}} \times \mathbf{u} - \frac{1}{\rho} \frac{\partial (\rho \overline{\mathbf{u}' u'_3})}{\partial z}, \quad (2)$$

where p is the pressure, ρ is the air density, f is the Coriolis parameter, and u_3 is the vertical velocity component. An analytically tractable model can be obtained as follows. First Eq. (2) is integrated from the surface $z = 0$ to an altitude $z = h$ in the mixed layer. Second, horizontal advection of momentum is neglected; that is, a ‘‘single-column model’’ approximation is made. Third, the surface eddy momentum flux is represented in terms of a standard Monin-Obukhov bulk parameterisation with drag coefficient c_d . Finally, the eddy momentum flux from above $z = h$ is expressed in terms of a ‘‘finite-differenced’’ eddy diffusion:

$$\overline{\mathbf{u}' u'_3} = -\frac{K}{h} (\mathbf{U} - \mathbf{u}), \quad (3)$$

where K is a kinematic eddy viscosity and \mathbf{U} represents the wind vector above $z = h$. The resulting differential equation can be expressed

$$\frac{d\mathbf{u}}{dt} = \mathbf{F} - \frac{c_d}{h} w \mathbf{u} - \frac{K}{h^2} \mathbf{u}, \quad (4)$$

where we have defined the quantity

$$\mathbf{F} = -\frac{1}{\rho} \nabla p - f \hat{\mathbf{k}} \times \mathbf{u} + \frac{K}{h^2} \mathbf{U}. \quad (5)$$

For the sake of convenience, we will assume that \mathbf{F} does not depend on \mathbf{u} ; in particular, we assume that the geostrophic residual between the pressure gradient force and the Coriolis force does not depend on the wind vector \mathbf{u} . Away from the equator, this approximation is similar to a small Rossby number approximation. Finally, we will assume that the forcing \mathbf{F} is fluctuating around some mean value:

$$F_u(t) = \langle F_u \rangle + \Sigma \dot{W}_1(t) \quad (6)$$

$$F_v(t) = \Sigma \dot{W}_2(t), \quad (7)$$

where the fluctuations are taken to be isotropic and white in time:

$$\langle \dot{W}_i(t_1) \dot{W}_j(t_2) \rangle = \delta_{ij} \delta(t_1 - t_2), \quad (8)$$

(where angle brackets denote ensemble averaging) with a strength that is tuned by the parameter Σ . Note that as by definition the average cross-mean wind is zero, the average of F_v must also be zero. The resulting equations for u and v read

$$\dot{u} = \langle F_u \rangle - \frac{c_d}{h} w u - \frac{K}{h^2} u + \Sigma \dot{W}_1 \quad (9)$$

$$\dot{v} = -\frac{c_d}{h} w v - \frac{K}{h^2} v + \Sigma \dot{W}_2. \quad (10)$$

Equations (9)-(10) are a stochastic differential equation (SDE) for the surface wind vector (Gardiner, 1997). The surface drag force depends on the wind speed $w = \sqrt{u^2 + v^2}$, the depth h of the atmospheric layer considered (taken as in Monahan (2004b) to be 80 m), and the drag coefficient c_d . In general, non-neutral stratification of the boundary layer and modification of the local sea state by surface winds both result in a dependence of c_d on w (through the Obukhov length in the first instance and the roughness length in the second). Furthermore, other factors such as surface surfactants and remotely generated swell introduce variations in the drag coefficient that are unrelated to the local winds. For simplicity, we will neglect the effects of stratification and swell and consider the parameterisation of the neutral drag coefficient for fully developed seas introduced by Taylor and Yelland (2001), as modified in Fairall et al. (2003) to include a correction for flow over an aerodynamically smooth surface during conditions of light winds. The dependence of the neutral drag coefficient on the surface wind speed remains a subject of active research (e.g. Jones and Toba (2001); Fairall et al. (2003)), and questions remain as to its precise formulation. Calculations using different expressions for the wind speed dependence of the drag coefficient (not shown) demonstrate that the following results are not qualitatively sensitive to which of the various parameterisations of c_d suggested in the literature are used.

One of Einstein's major insights in his *annus mirabilis* (Einstein, 1956) was that the pdf of the solutions of a SDE satisfies a diffusion equation now known as a Fokker-Planck equation (e.g. Gardiner, 1997). In particular, the stationary joint pdf of u and v , $p(u, v)$, associated with the SDE (9) - (10) satisfies the Fokker-Planck equation:

$$0 = \frac{\partial}{\partial u} \left(\langle F_u \rangle - \frac{c_d}{h} w u - \frac{K}{h^2} u \right) p + \frac{\partial}{\partial v} \left(-\frac{c_d}{h} w v - \frac{K}{h^2} v \right) p + \frac{\Sigma^2}{2} \left(\frac{\partial^2 p}{\partial u^2} + \frac{\partial^2 p}{\partial v^2} \right), \quad (11)$$

which has the solution

$$p(u, v) = \mathcal{N}_1 \exp \left(\frac{2}{\Sigma^2} \left\{ \langle F_u \rangle u - \frac{K}{2h^2} (u^2 + v^2) - \frac{1}{h} \int_0^{\sqrt{u^2 + v^2}} c_d(w') w'^2 dw' \right\} \right), \quad (12)$$

where \mathcal{N}_1 is a normalisation constant. Note that the pdf (12) is symmetric in v , so

$$\int_{-\infty}^{\infty} \int_{-\infty}^{\infty} u v p(u, v) du dv = 0. \quad (13)$$

Fluctuations in u and v are therefore uncorrelated, although they are not independent (i.e. $p(u, v)$ does not factor as the product of the marginal distributions of u and v). Independence of u and v holds only in the unphysical case of linear surface drag, $c_d = k/w$. Note also that the pdf (12) is bivariate Gaussian in the limit of linear drag; nonzero skewness in the vector winds is a consequence of nonlinear surface drag.

The marginal pdf of u , $p(u)$, follows from integrating the pdf (12) over v ; Figure 3 contours $\text{mean}(u)$, $\text{std}(u)$ and $\text{skew}(u)$ as functions of $\langle F_u \rangle$ and Σ . The ranges of these parameters were chosen so that the ranges of the simulated moments were quantitatively similar to those observed (Figure 1), and a typical boundary-layer value of $K = 1 \text{ m}^2 \text{ s}^{-1}$ was used. By construction, $\text{mean}(w) > 0$ for all parameter values. More significantly, $\text{skew}(w)$ is everywhere negative, and for most parameter values becomes more negative as $\text{mean}(w)$ becomes more positive. In this simple stochastic boundary layer model, as in the observations, the mean and skewness of the vector wind are anticorrelated.

An intuitive understanding of the relationship between the mean and skewness of the surface wind components is straightforward. Consider the atmospheric surface layer subject to zonal forcing F_u with zero mean and with fluctuations that are equally as likely to be positive as negative. By symmetry, the mean and skewness of the resulting zonal wind will both be zero. Now suppose that the zonal forcing F_u has a nonzero mean, which by construction is positive, so that $\text{mean}(u)$ will be positive. Because of the nonlinear surface drag, positive anomalies in u will be subject to stronger friction than negative anomalies. Consequently, a positive perturbation in the forcing will produce a weaker response than a negative perturbation of the same magnitude, and the symmetric fluctuations will produce an asymmetric response. In particular, a tail toward slower zonal

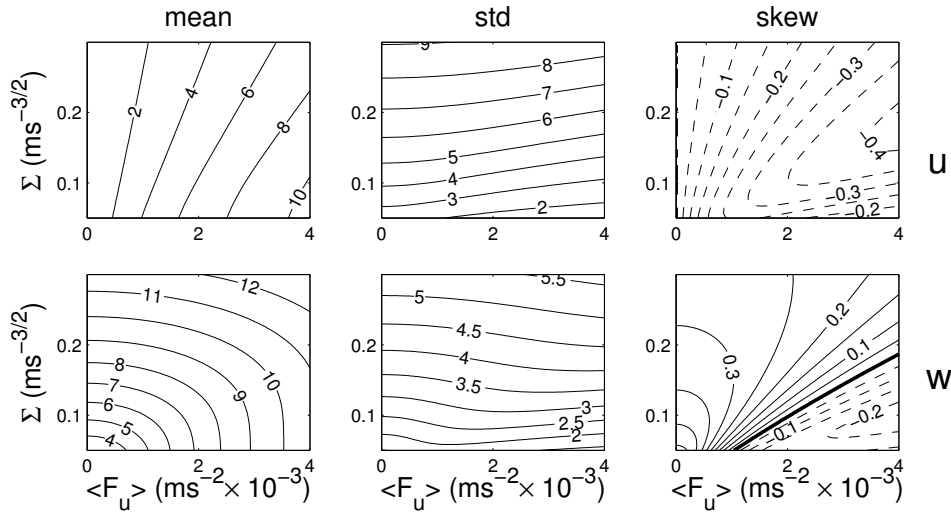


Figure 3: Contours of the mean, standard deviation, and skewness of the along-mean wind component u and wind speed w from the stochastic boundary layer model (9)-(10), as functions of the forcing mean $\langle F_u \rangle$ and fluctuation strength Σ .

winds will develop in the distribution, so the zonal wind will be negatively skewed. As the mean of F_u increases, the asymmetry in drag between positive and negative u anomalies will also increase, and so the skewness will become more strongly negative. In this manner, the nonlinear surface drag results in the anticorrelation of the mean and skewness fields of zonal surface winds.

An analytic expression for the pdf of w can be obtained from Eqn. (12) as follows: moving to polar coordinates,

$$u = w \cos \theta \quad (14)$$

$$v = w \sin \theta \quad (15)$$

such that the average value of θ is zero (by construction), conservation of probability under a coordinate change requires that the joint pdf $p(w, \theta)$ must satisfy

$$p(u, v) du dv = p(w \cos \theta, w \sin \theta) w dw d\theta = p(w, \theta) dw d\theta. \quad (16)$$

Thus,

$$p(w, \theta) = \mathcal{N}_1 w \exp \left(\frac{2}{\Sigma^2} \left\{ \langle F_u \rangle w \cos \theta - \frac{K}{2h^2} w^2 - \frac{1}{h} \int_0^w c_d(w') w'^2 dw' \right\} \right). \quad (17)$$

The marginal distribution $p(w)$ for the wind speed w is obtained by integrating $p(w, \theta)$ over the angle θ . Performing the integral, we obtain the closed-form expression:

$$p(w) = \mathcal{N}_1 w I_0 \left(\frac{2 \langle F_u \rangle w}{\Sigma^2} \right) \exp \left(-\frac{2}{\Sigma^2} \left[\frac{K}{2h^2} w^2 + \frac{1}{h} \int_0^w c_d(w') w'^2 dw' \right] \right). \quad (18)$$

where I_0 is the modified Bessel function of order zero.

The mean, standard deviation, and skewness of wind speed w from Eqn. (18) are contoured as functions of $\langle F_u \rangle$ and Σ in the lower panels of Figure 3. The mean wind speed is an increasing function of both $\langle F_u \rangle$ and Σ . The standard deviation of w is determined primarily by Σ , displaying only a weak dependence on $\langle F_u \rangle$. Finally, skew(w) depends on both $\langle F_u \rangle$ and Σ ; in particular, the skewness of w is negative when the forcing has a large mean but relatively small fluctuations; as the magnitude of the fluctuations increases, the skewness eventually becomes positive.

Inspection of Figure 1 indicates that in general the surface wind speed distribution is negatively skewed in the eastern equatorial Pacific and along the equatorward flanks of the subtropical highs, regions characterised by relatively high mean wind speeds and relatively low variability. The regions of strongest positive skewness are the Northern Hemisphere midlatitudes, characterised by intermediate mean wind speeds and strong variability. Finally, the Southern Ocean is characterised by high mean(w), intermediate std(w), and skew(w) close to zero. Qualitatively, the relationship between the spatial structures of the mean(w), std(w), and skew(w) fields is as predicted by the pdf (18).

The agreement of the relationships between moments from the observations and from the pdf (18) is most obvious in a plot of skew(w) as a function of mean(w)/std(w) (Figure 3). Like the associated curve for a Weibull distribution, this curve is concave upward and runs through the middle of the observed joint pdf of mean(w)/std(w) with skew(w), taking positive values when the ratio mean(w)/std(w) is small and negative values when this ratio is large. In fact, for values of this ratio of approximately 2 and greater, the curve predicted by the stochastic boundary layer model is at least as good a representation of the observed joint pdf as is the Weibull curve. For lower values of the ratio, however, the performance of the model is not so good: the predicted skewness does not take values greater than approximately 0.5, considerably below the maximum observed skewness. It is evident that while both the Weibull distribution and the pdf (18) capture aspects of the relationships between moments observed in sea surface wind speeds, neither is entirely accurate. It should be emphasised, however, that the pdf (18) arises from physical arguments via a clear series of approximations, while the Weibull characterisation of sea surface wind speeds is entirely empirical. The success of the Weibull distribution as a useful approximation to the distribution of w evidently arises because it imposes the constraints on the relationship between mean(w), std(w), and skew(w) that are required by the physics of the atmospheric boundary layer.

An intuitive understanding of the dependence of mean(w), std(w), and skew(w) on $\langle F_u \rangle$ and Σ is straightforward. An increase in $\langle F_u \rangle$ will lead to an increase in mean(u), and consequently to an increase in the mean wind speed. The joint pdf of u and v becomes broader as Σ increases; this shift of probability mass away from the origin increases both the mean amplitude w of the vector wind and its variability. Finally, the skewness of w is determined by the width of the pdf of w relative to its mean value, i.e. the ratio mean(w)/std(w). For smaller values of this ratio, the distribution $p(u, v)$ is concentrated around the origin and the distribution of the magnitude w has a tail toward larger values, so skew(w) is positive. Conversely, for larger values of this ratio, the joint pdf $p(u, v)$ is centred away from the origin. Because of the anticorrelation of mean(u) and skew(u), $p(u, v)$ will be characterised by a tail extending toward the origin. As the mass of $p(u, v)$ is concentrated away from the origin, this tail will also be present in the marginal pdf of w , so skew(w) will be negative. The fact that the pdf (18) can become negatively skewed is a consequence of the anticorrelation between the mean and skewness of the vector wind components, which can be understood to arise because of the nonlinearity of the surface drag law. For a linear drag law ($c_d = k/w$), for which the vector winds are Gaussian, the skewness of w from pdf (18) (not shown) is always positive.

4 Sea Surface Wind pdfs: Empirical Model

While the stochastic boundary layer model (9)-(10) provides physical insight into the pdf of sea surface winds, it is too simple to be quantitatively accurate. A more quantitatively accurate empirical model can be obtained by assuming that the fluctuations of u and v are independent and isotropic (with standard deviation σ), such that v is a zero-mean Gaussian:

$$p(v) = \frac{1}{\sqrt{2\pi\sigma^2}} \exp\left(-\frac{v^2}{2\sigma^2}\right), \quad (19)$$

while u has non-zero mean \bar{u} , skewness ν , and kurtosis κ :

$$p(u) = \frac{1}{\sqrt{2\pi\sigma^2}} \left[1 + \frac{\nu}{6} H_3 \left(\frac{u - \bar{u}}{\sigma} \right) + \frac{\kappa}{24} H_4 \left(\frac{u - \bar{u}}{\sigma} \right) \right] \exp \left(-\frac{(u - \bar{u})^2}{2\sigma^2} \right), \quad (20)$$

where $H_3(x) = x^3 - 3x$ and $H_4(x) = x^4 - 6x^2 + 3$ are respectively the third- and fourth-order Hermite polynomials. The kurtosis of a variable x is defined as its normalised fourth-order moment,

$$\text{kurt}(x) = \frac{\text{mean}((x - \text{mean}(x))^4)}{\text{std}^4(x)} - 3. \quad (21)$$

The distribution (20) is a Gram-Charlier expansion of a Gaussian (Johnson et al., 1994); a drawback of such expansions is that the resulting distribution is not guaranteed to be positive definite. In practice, the Gram-Charlier densities only ever become slightly negative for the parameter values used in the present analysis.

Having assumed that the pdfs of u and v are independent, their joint pdf is simply the product of the marginal pdfs (19) and (20). This joint pdf can be integrated over the wind direction to yield the marginal pdf for the wind speed w . This pdf, denoted $D(\nu, \kappa)$, can be expressed analytically in terms of a combination of Hermite polynomials and modified Bessel functions (Monahan, 2005a). An empirical pdf of this form with $\nu = \kappa = 0$ was studied in Cakmur et al. (2004); the distribution $D(0, 0)$ will then also be denoted the CMT distribution.

To determine the accuracy of the $D(\nu, \kappa)$ distribution in characterising the probability distribution of sea surface wind speeds, \bar{u} and σ^2 were estimated from the SeaWinds surface wind data. Because fluctuations in the along- and cross-mean wind directions are not exactly isotropic, σ was estimated as

$$\sigma = \left[\frac{1}{2} (\text{std}^2(u) + \text{std}^2(v)) \right]^{1/2}. \quad (22)$$

We take advantage of the dependence of the higher-order moments of the vector wind on the lower-order moments by estimating statistical parameterisations of ν and κ as functions of \bar{u} and σ^2 , denoted respectively $\nu_{eff}(\bar{u}, \sigma)$ and $\kappa_{eff}(\bar{u}, \sigma)$. These statistical models are constructed from the observed moment fields using feed-forward neural networks (e.g. Hsieh and Tang, 1998), which are powerful tools for nonlinear, nonparametric function estimation.

Fields of $\text{mean}(w)$, $\text{std}(w)$, and $\text{skew}(w)$ predicted from the CMT and $D(\nu_{eff}, \kappa_{eff})$ distributions are displayed in Figure 4; it must be emphasised that both these empirical distributions make use of precisely the same input information: the mean and standard deviation of the vector wind. The CMT distribution generally underestimates $\text{mean}(w)$ and overestimates $\text{std}(w)$; more significantly, it predicts $\text{skew}(w) > 0$ everywhere. The biases in $\text{mean}(w)$ and $\text{std}(w)$ are reduced (by $\sim 40\%$ on average) in the $D(\nu_{eff}, \kappa_{eff})$ distribution relative to the CMT distribution. Furthermore, $D(\nu_{eff}, \kappa_{eff})$ predicts bands of negative $\text{skew}(w)$ over the tropics and near-zero $\text{skew}(w)$ over the Southern Ocean.

The CMT distribution is unable to account for negative wind speed skewness in the tropics and for the band of near-zero skewness over the Southern Ocean. Note that the CMT distribution assumes Gaussian vector winds; consistent with the results of the stochastic boundary-layer model, non-Gaussian structure in u is required to account for the $\text{skew}(w)$ field over the tropics and the Southern Ocean.

This analysis demonstrates two important points: firstly, that the moments of the scalar sea surface wind speed can be quite accurately predicted given a knowledge of the moments of the vector wind, and secondly that the higher order moments of the vector wind can accurately be parameterised in terms of the lower moments, as was suggested in Monahan (2004b). The gridscale-averaged vector surface wind is a standard atmospheric general circulation model field, and parameterisations exist of the gridscale variability of the vector wind (Cakmur et al., 2004); these quantities can be used as input to the parameterisation of the pdf of w presented in this study to improve representations of grid-scale averaged fluxes (which are in general not equal to the fluxes associated with grid-scale average winds (e.g. Mahrt and Sun, 1995)).

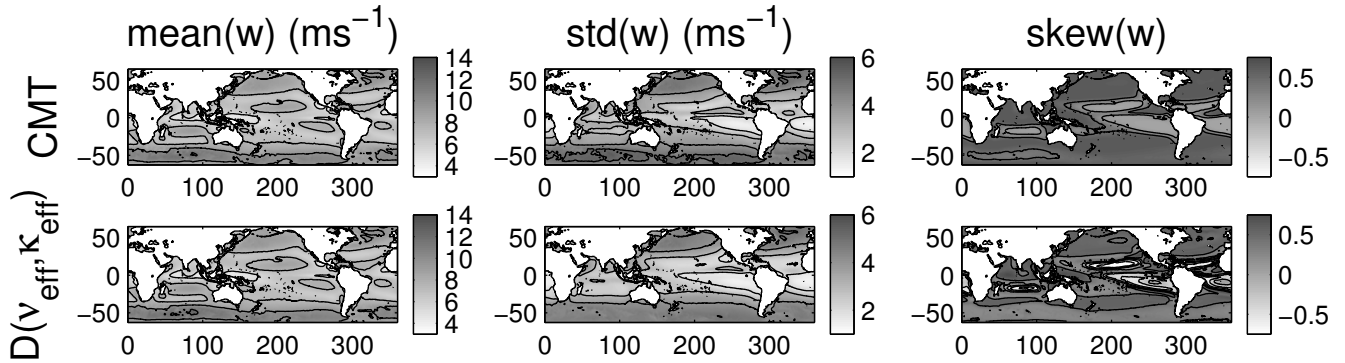


Figure 4: Mean, standard deviation, and skewness fields from the CMT and $D(v_{eff}, \kappa_{eff})$ distributions.

5 Conclusions

A primary motivation for the study of the probability distribution of sea surface winds from the perspective of climate studies is the role these distributions play in the computation of spatially and/or temporally averaged air/sea fluxes of momentum, energy, freshwater, and chemical constituents (e.g. Jones and Toba, 2001). This study has discussed both theoretical and empirical parameterisations of sea surface wind pdfs. In particular, an empirical model of $p(w)$ has been proposed which depends on averaged vector quantities of the kind naturally produced by GCMs. The incorporation of these pdfs into parameterisations of air/sea fluxes in GCMs, as discussed in Cakmur et al. (2004), presents the possibility of improving the representation of the surface fluxes that are at the heart of the coupled physical-biogeochemical dynamics of the climate system.

Acknowledgements

This research was supported by the Natural Sciences and Engineering Research Council of Canada, by the Canadian Foundation for Climate and Atmospheric Sciences, and by the Canadian Institute for Advanced Research Earth System Evolution Program.

References

- Bourassa, M. A., D. M. Legler, J. J. O'Brien, and S. R. Smith, 2003: SeaWinds validation with research vessels. *J. Geophys. Res.*, **108**, doi:10.1029/2001JC001028.
- Cakmur, R., R. Miller, and O. Torres, 2004: Incorporating the effect of small-scale circulations upon dust emission in an atmospheric general circulation model. *J. Geophys. Res.*, **109**, D07201.
- Ebuchi, N., H. C. Graber, and M. J. Caruso, 2002: Evaluation of wind vectors observed by QuikSCAT/SeaWinds using ocean buoy data. *J. Atmos. Ocean. Tech.*, **19**, 2049–2062.
- Einstein, A., 1956: *Investigations on the Theory of Brownian Movement*. Dover, New York.
- Fairall, C. W., E. F. Bradley, J. E. Hare, A. A. Grachev, and J. B. Edson, 2003: Bulk parameterization of air-sea fluxes: Updates and verification for the COARE algorithm. *J. Climate*, **16**, 571–591.

- Gardiner, C. W., 1997: *Handbook of Stochastic Methods for Physics, Chemistry, and the Natural Sciences*. Springer, 442 pp.
- Hsieh, W. W. and B. Tang, 1998: Applying neural network models to prediction and data analysis in meteorology and oceanography. *Bull. Amer. Met. Soc.*, **79**, 1855–1870.
- Isemer, H. and L. Hasse, 1991: The scientific Beaufort equivalent scale: Effects on wind statistics and climatological air-sea flux estimates in the North Atlantic Ocean. *J. Climate*, **4**, 819–836.
- Jet Propulsion Laboratory, 2001: SeaWinds on QuikSCAT Level 3: Daily, Gridded Ocean Wind Vectors. Technical Report JPL PO.DAAC Product 109, California Institute of Technology.
- Johnson, N., S. Kotz, and N. Balakrishnan, 1994: *Continuous univariate distributions*, volume 1. Wiley, New York, 756 pp.
- Jones, I. S. and Y. Toba, eds., 2001: *Wind Stress Over the Ocean*. Cambridge University Press, Cambridge, 307 pp.
- Kelly, K. A., 2004: Wind data: A promise in peril. *Science*, **303**, 962–963.
- Mahrt, L. and J. Sun, 1995: The subgrid velocity scale in the bulk aerodynamic relationship for spatially averaged scalar fluxes. *Mon. Weath. Rev.*, **123**, 3032–3041.
- Meissner, T., D. Smith, and F. Wentz, 2001: A 10 year intercomparison between collocated Special Sensor Microwave Imager oceanic surface wind speed retrievals and global analyses. *J. Geophys. Res.*, **106**, 11731–11742.
- Monahan, A. H., 2004a: Low-frequency variability of the statistical moments of sea-surface winds. *Geophys. Res. Lett.*, **31**, doi:10.1029/2004GL019599.
- 2004b: A simple model for the skewness of global sea-surface winds. *J. Atmos. Sci.*, **61**, 2037–2049.
- 2005a: The probability distribution of sea surface wind speeds. Part I: Theory and SeaWinds observations. *J. Climate*, **submitted**.
- 2005b: The probability distribution of sea surface wind speeds. Part II: Dataset intercomparison and seasonal variability. *J. Climate*, **submitted**.
- Petersen, E. L., N. G. Mortensen, L. Landberg, J. Højstrup, and H. P. Frank, 1998: Wind power meteorology. Part I: Climate and turbulence. *Wind Energy*, **1**, 25–45.
- Sura, P., 2003: Stochastic analysis of Southern and Pacific ocean sea surface winds. *J. Atmos. Sci.*, **60**, 654–666.
- Sura, P. and P. Sardeshmukh, 2004: Stochastic analysis of sea surface wind vectors: the role of multiplicative noise. *J. Atmos. Sci.*, **submitted**.
- Taylor, P. K. and M. J. Yelland, 2001: The dependence of sea surface roughness on the height and steepness of the waves. *J. Phys. Oceanogr.*, **31**, 572–590.
- Thompson, K., R. Marsden, and D. Wright, 1983: Estimation of low-frequency wind stress fluctuations over the open ocean. *J. Phys. Oceanogr.*, **13**, 1003–1011.
- Wanninkhof, R., S. C. Doney, T. Takahashi, and W. R. McGillis: 2002, The effect of using time-averaged winds on regional air-sea CO₂ fluxes. *Gas Transfer at Water Surfaces*, M. A. Donelan, W. M. Drennan, E. S. Saltzman, and R. Wanninkhof, eds., American Geophysical Union, 351–356.